Inorganic Chemistry

Article

pubs.acs.org/IC

Probing the Role of Secondary versus Tertiary Amine Donor Ligands for Indium Catalysts in Lactide Polymerization

Kimberly M. Osten, Dinesh C. Aluthge, Brian O. Patrick, and Parisa Mehrkhodavandi*

Department of Chemistry, University of British Columbia, 2036 Main Mall, Vancouver, British Columbia V6T 1Z1, Canada

Supporting Information

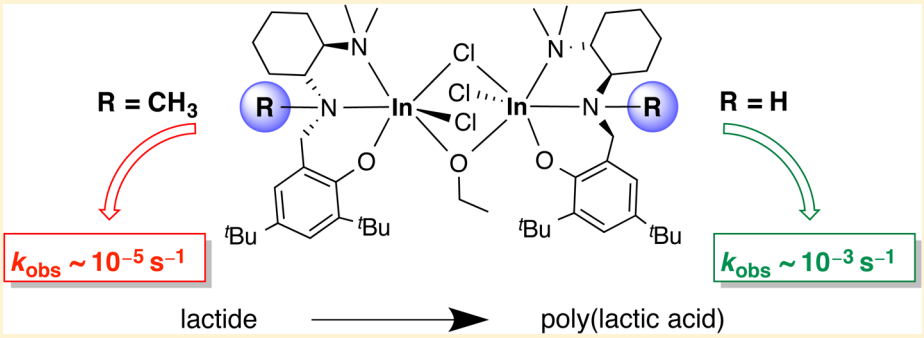

ABSTRACT: The role of the central amine donor in a previously reported dinuclear indium catalyst, $[N_{Me2}N_HO)InCl]_2(\mu$-Cl)(μ-OEt) (**1**), for the polymerization of lactide was investigated through experimental methods. The solid state structural data of a series of dimeric complexes related to **1**, including the previously reported bromide derivative $[(N_{Me2}N_HO)InBr](\mu$-Br)(μ-OEt) (**2**) and the newly synthesized methylated derivative $[(N_{Me2}N_{Me}O)InCl]_2(\mu$-Cl)($\mu$-OEt) (**6**), showed that weak hydrogen bonding may be present within some of these complexes in the solid state. The polymerization of *rac*-lactide with **2**, **6**, and a related achiral complex $[(L_H)InCl]_2(\mu$-Cl)(μ-OEt) (**8**) synthesized for this study indicates that hydrogen bonding may not influence the reactivity of these compounds. The nature of the central amine donor may play a role in tuning the reactivity of these types of catalysts. Catalysts with central secondary amine donors, such as complexes **1**, **2**, and **8**, are 2 orders of magnitude more reactive than those with central tertiary amine donors, such as complex **6**.

INTRODUCTION

Amine donors are a ubiquitous part of a vast array of ancillary ligands and have been used as excellent supports for Lewis acidic metal centers in the catalytic ring opening polymerization of lactide (LA) to form the biodegradable polymer poly(lactic acid) (PLA).[1] In particular, the amino-phenol proligand architecture has been used to support zinc and group 13 metals.[2,3]

We have investigated a family of diamino phenolate supports for zinc[4] and indium[5] catalysts for the ring opening polymerization of lactide. These proligands are related to the highly active diamino phenolate supported zinc catalyst $[(L_{Me})Zn(\mu$-OEt)$]_2$ (**A**) reported by Hillmyer and Tolman (Chart 1).[6] We showed that the analogous chiral zinc complex $(N_{Me2}N_{Me}O)Zn(OPh)$ (**B**) was unreactive in polymerization reactions and that the high reactivity of complex **A** can be attributed to the dissociation of the ethylene diamine linker and the formation of a reactive coordinatively unsaturated zinc center.[4] In contrast, the ligand set in **B** is not labile. Surprisingly, indium alkoxide complex $[(L_{Me})InCl]_2(\mu$-Cl)(μ-OEt) (**C**) bearing the labile ligand set is also inactive for lactide polymerization, indicating that ligand lability is not the deciding factor in the reactivity of these indium complexes.[5b]

Given our reports of highly active dinuclear indium complexes,[7] such as $[(N_{Me2}N_HO)InCl]_2(\mu$-Cl)($\mu$-OEt) (**1**),[5d] as catalysts for the ring opening polymerization (ROP) of cyclic esters (Chart 2), we were keen to explore the role of the amine donors in the reactivity of our complexes.[5] A recent mechanistic investigation of this system shows that complexes such as **1** are dinuclear both in the solid state and in solution and remain dinuclear during the polymerization reaction.[8] More recently, we have disclosed the results of computational studies with this system, where we confirmed both the dinuclear nature of the catalyst during polymerization as well as the importance of a dinuclear catalyst in the selectivity of the system.[9]

During these investigations, it came to our attention that hydrogen bonding between the secondary amine donor and the terminal chloride may be playing a structural role in the stability of these dinuclear catalysts and may in part explain the reactivity difference between catalysts with tertiary and secondary amine donors. The importance of the nature of the amine has been previously explored for other kinds of reactivity.[10] Herein we present our exploration of the role of secondary versus tertiary amines in our ligand architecture and the impact, if any, of hydrogen bonding in these systems during the ring opening polymerization of lactide.

Received: June 27, 2014
Published: August 27, 2014

   dx.doi.org/10.1021/ic501529f | *Inorg. Chem.* 2014, 53, 9897−9906

Chart 1. Previously Reported Diaminophenolate-Supported Zinc and Indium Complexes A,[6] B,[4] and C[5b]

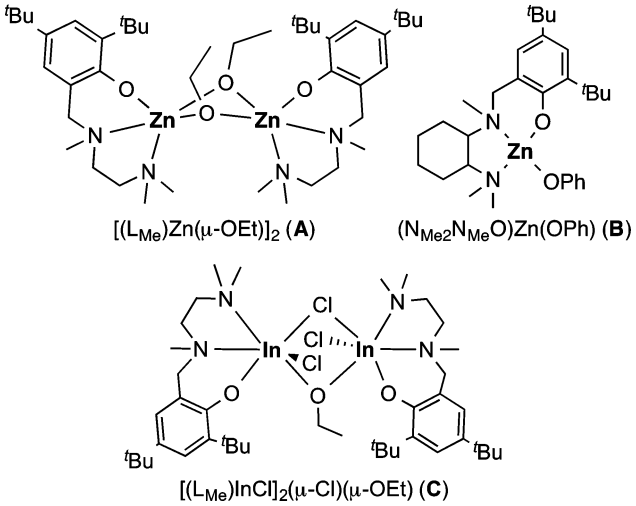

Chart 2. Previously Reported Chiral Dinuclear Indium Catalysts for ROP of Lactide[5c,d,8]

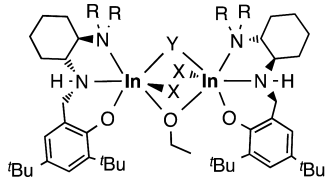

[(N$_R$N$_H$O)InX]$_2$(μ-Y)(μ-OEt)
(**1**) R = Me, X = Y = Cl
(**2**) R = Me, X = Y = Br
(**3**) R = Me, X = I, Y = OH
(**4**) R = ^{n}Pr, X = Cl, Y = OH
(**4'**) R = ^{n}Pr, X = Y = Cl

RESULTS AND DISCUSSION

Synthesis of Indium Complexes. We can synthesize an analogue of complex **1** with a tertiary amine as the central donor of the ligand. The racemic methylated proligand (±)-**H-(N$_{Me2}$N$_{Me}$O)** can be prepared according to previously published procedures.[4,11] The proligand is first deprotonated with benzyl potassium to yield K(N$_{Me2}$N$_{Me}$O), which is reacted *in situ* with InCl$_3$ to yield the dichloro indium complex (N$_{Me2}$N$_{Me}$O)InCl$_2$ (**5**) (Scheme 1).[5d] The ^{1}H NMR spectrum of **5** shows characteristic N−C*H*$_2$ methylene signals of the ligand backbone as two doublets at 4.17 and 3.86 ppm (Figure S1, Supporting Information). Signals for three inequivalent N−C*H*$_3$ methyl protons are observed at 2.82, 2.62, and 2.29 ppm. This asymmetry is present in similar compounds reported by our group.[4]

Reaction of complex **5** with 0.98 equiv of NaOEt in THF forms the dinuclear complex [(N$_{Me2}$N$_{Me}$O)InCl]$_2$(*μ*-Cl)(*μ*-OEt) (**6**) (Scheme 1). The choice of solvent for this reaction is important and can have an impact on the ease of purification: parent complex [(N$_{Me2}$N$_H$O)InCl]$_2$(*μ*-Cl)(*μ*-OEt) (**1**) is soluble in toluene, while **6** is insoluble in toluene and sparingly soluble in THF, making removal of the NaCl byproduct of this reaction difficult.[5d] Reasonable yields (70%) of complex **6** can be obtained by dissolution and filtration of the crude precipitate in CH_2Cl_2. The ^{1}H NMR spectrum of **6** shows signals for the N−C*H*$_2$ protons as doublets at 4.75 and 3.38 ppm flanking the −OC*H*$_2$CH$_3$ protons, which appear as overlapping multiplets centered at 4.41 ppm (Figure S3, Supporting Information). Each of these three signals corresponds to one proton. This pattern is consistent with a single ethoxide ligand bridging the indium centers similar to complex **1**.[5d]

Scheme 1. Synthesis of Complex 6

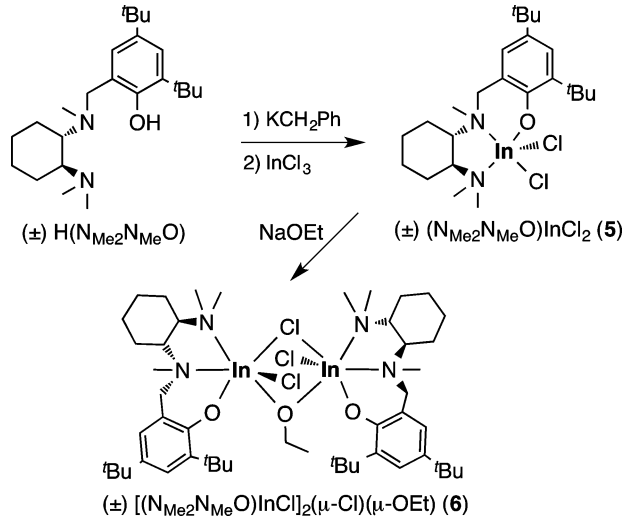

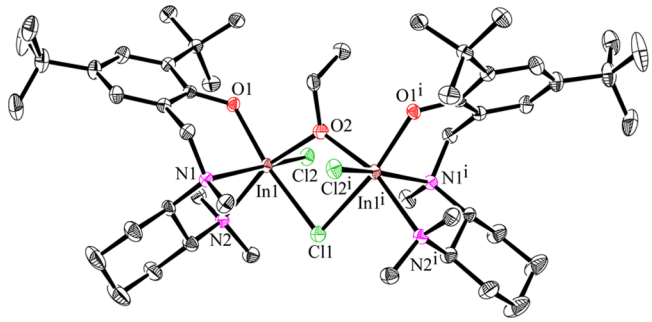

Figure 1. Molecular structure of complex **6**. H atoms, solvent molecules, and disorder of the OEt group removed for clarity.

The solid state structure of complex **6**, determined by single-crystal X-ray diffraction, shows a homochiral dinuclear indium complex with (*R*,*R*) ligand configuration at each octahedral indium center (Figure 1). There is a 2-fold rotational axis through the central bridging chloride, and the ethoxide is disordered about this axis with an occupancy of 0.5 for each site. There is a "cis" relationship between the phenoxy groups of the ligand; i.e., they are on the same side of the dimeric structure. This configuration is observed for all related compounds generated from racemic ligands in this family.[5b−d,8]

As mentioned above, we have previously reported the synthesis of a related indium complex, [(L$_{Me}$)InCl]$_2$(*μ*-Cl)(*μ*-OEt) (**C**), for the polymerization of lactide (Chart 1).[6] We can synthesize the analogous complex with a secondary amine as the central donor (**L$_H$**) via a similar route (Scheme 2).[12] Deprotonation of **L$_H$** with KO^{t}Bu followed by salt metathesis with InCl$_3$ yields (L$_H$)InCl$_2$ (**7**). The ^{1}H NMR spectrum of **7** is similar to complex **C** and shows the central N-C*H*$_2$ protons of the backbone as two multiplets at 4.78 and 3.86 ppm (Figure S7, Supporting Information). The N−C*H*$_3$ methyl protons are observed as two inequivalent signals at 2.69 and 2.40 ppm, with the N-*H* proton observed between them at 2.54 ppm. Salt metathesis reaction of **7** with NaOEt yields [(L$_H$)InCl)]$_2$(*μ*-Cl)(*μ*-OEt) (**8**). The ^{1}H NMR spectrum of **8** shows the N-C*H*$_2$ protons of the backbone as two doublets at 5.04 and 3.63 ppm, which flank the −OC*H*$_2$CH$_3$ protons that appear as overlapping multiplets centered at 4.44 ppm (Figure S9, Supporting Information). As with complex **6**, these signals correspond to

dx.doi.org/10.1021/ic501529f | Inorg. Chem. 2014, 53, 9897−9906

Scheme 2. Synthesis of Complex 8

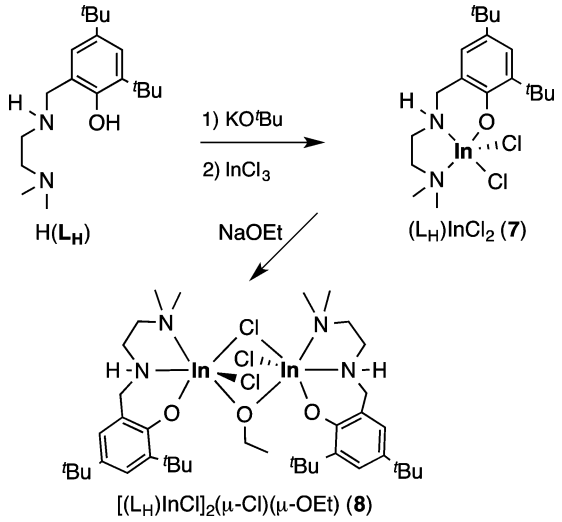

one proton each, confirming the presence of a single ethoxide bridging ligand in this complex.

Single crystals of complex **8** were grown from a saturated solution of the complex in acetonitrile, and the solid state structure was determined by single-crystal X-ray diffraction. It shows a dinuclear indium complex with a "cis" relationship between the phenoxy groups of the ligand, similar to complex **1** (Figure 2).

In order to determine if H--X hydrogen bonding plays a role in stabilizing the dimeric structure of these types of catalysts, we obtained an improved solid state structure for compound **1** and also acquired the solid state structure of the previously reported[5c] bromide complex $[(N_{Me2}N_HO)InBr]_2(\mu\text{-Br})(\mu\text{-OEt})$ (**2**) by single-crystal X-ray diffraction (Figure 2). The compounds crystallize as homochiral dimers with "cis" relationships between the two ligands of the dimer as seen for previous compounds. Both the (*RR*/*RR*) and (*SS*/*SS*) dimers are observed as two separate molecules in the unit cell. The (*RR*/*RR*) dimers are shown in Figure 2.

Inspection of the structural data for the complexes **1**−**4**, **6**, and **8** allows for a comparison of the hydrogen bonding parameters for these complexes (Table 1). In addition to the H−X (d) and N_1−X (D) bond distances and the N−H−X bond angle (θ), Table 1 includes the ratio between the observed H−X distances and the sum of the van der Waals radii of the H and X atoms (R_{HX}).[13] This value normalizes the differences between the van der Waals radii of the halogens and provides a useful way to compare the extent of hydrogen bonding in complexes with different halogen acceptors. A value of 1 for R_{HX} would indicate the hydrogen bond distance is equal to the sum of the van der Waals radii of the participating atoms, and thus the H-bond would be very weak or nonexistent. Therefore, lower R_{HX} numbers would indicate stronger hydrogen bonding is present in the system.

Several comprehensive studies of crystallographic databases provide tabulated hydrogen bonding parameters for NH−X type hydrogen bonds. The N−X distances range from 3.3 to 3.7 Å, and the H−X distances range from 2.5 to 2.9 Å. The R_{HX} values are 0.85, 0.87, and 0.92 for chloro, bromo, and iodo acceptors, respectively.[13,14] Our parameters for the chloro (**1**), bromo (**2**), and iodo (**3**) analogues with the parent ligand are in line with the literature values and show a general trend of decreasing hydrogen bond strength in moving from chloro to iodo acceptors, as

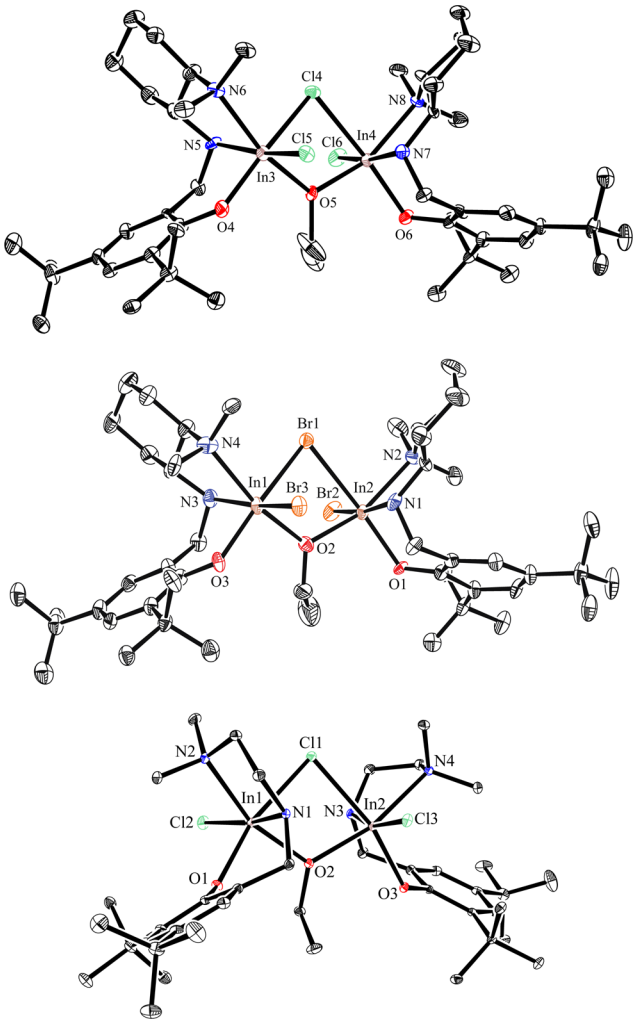

Figure 2. Molecular structures of complexes **1** (top), **2** (middle), and **8** (bottom). H atoms, solvent molecules, and the (*SS*/*SS*) dimer (for complexes **1** and **2**) omitted for clarity.

expected. However, complex **4**, where the N-Me_2 is replaced with a bulkier N-(^{n}Pr)$_2$ group, has slightly longer bond distances and an R_{HX} value close to 1, suggesting that this complex may only have very weak hydrogen bonds. The achiral complex **8** has larger H−X and R_{HX} values than complex **1**, suggesting that this complex may have weaker hydrogen bonding than its chiral analogue. Thus, it is possible to compare complexes with a range of hydrogen bonding from fairly strong (**1**), to intermediate (**2**), to weak (**3**−**4**, **8**) and finally to nonexistent (**6**).

In interpreting this data, however, it is important to note the structural differences between some of these complexes. The second bridging ligand between complexes **1** and **2**, which have ethoxy and halo bridging ligands, is different from complexes **3** and **4**, with ethoxy and hydroxy bridging ligands (see Chart 2). Indeed complex **4** is further differentiated by the fact that it crystallizes symmetrically, with both sides of the dimer being equivalent. Unfortunately, structural data for the exact iodo and propyl analogues of complex **1** are unavailable. Therefore, it is unclear whether the weak H-bonding seen in complexes **3** and **4** is a consequence of structural changes due to the hydroxy bridging ligand or is due to the direct influence of the iodo or propyl groups.

In order to probe the effects of changing the strength of the hydrogen bonding without changing the sterics or electronics of

dx.doi.org/10.1021/ic501529f | Inorg. Chem. 2014, 53, 9897−9906

Table 1. Selected Solid State Structural Data for Related Indium Catalysts[a]

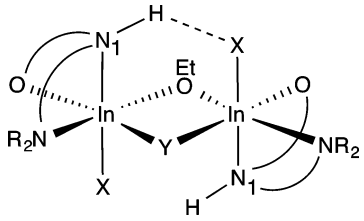

complex	X	N_1–X (Å)	H–X (Å)	N_1–H–X (deg)	R_{HX}
1[b]	Cl	3.416 (4.517)	2.445 (3.788)	163.5 (131.8)	0.83 (1.28)
2[b]	Br	3.535 (4.605)	2.662 (3.938)	160.9 (132.8)	0.87 (1.29)
3[c]	I	3.803 (3.790)	2.926 (3.045)	149.5 (150.1)	0.93 (0.96)
4	Cl	3.730	2.830	163.6	0.96
8	Cl	3.454 (4.518)	2.591 (3.641)	147.2 (150.4)	0.88 (1.23)
6	Cl	4.487			

[a]Values in parentheses are from the second half of the molecule in nonsymmetric structures. [b]Values are for the (*RR/RR*) molecule in the unit cell. [c]Values not in parentheses are an average of two measurements because of structural disorder in the ligand on one-half of the molecule.

Table 2. Observed Rates of Ring Opening Polymerization of *rac*-LA for Selected Indium Alkoxide Catalysts

	complex	R_{HX}[a]	k_{obs} ($\times 10^{-3}$ s^{-1})[d]	k_p (M^{-1} s^{-1})
1	$[(N_{Me2}N_HO)InCl]_2(\mu\text{-Cl})(\mu\text{-OEt})$[5d]	0.83 (1.28)[b]	1.7	0.57(5)
2	$[(N_{Me2}N_HO)InBr]_2(\mu\text{-Br})(\mu\text{-OEt})$	0.87 (1.29)[b]	4.8	2.2(1)
3	$[(N_{Me2}N_HO)InI]_2(\mu\text{-OH})(\mu\text{-OEt})$[8]	0.93 (0.96)[c]	3.5	1.5(1)
4′	$[(N_{nPr2}N_HO)InCl]_2(\mu\text{-Cl})(\mu\text{-OEt})$[5b]	0.96[e]	2.1	
8	$[(L_H)InCl]_2(\mu\text{-Cl})(\mu\text{-OEt})$	0.88 (1.23)	0.76	
6	$[(N_{Me2}N_{Me}O)InCl]_2(\mu\text{-Cl})(\mu\text{-OEt})$		0.012	
C	$[(L_{Me})InCl]_2(\mu\text{-Cl})(\mu\text{-OEt})$[5b]		0.011	

[a]Values in parentheses are from the second half of the molecule in nonsymmetric structures. [b]Values are for the (*RR/RR*) molecule in the unit cell. [c]Values not in parentheses are an average of two measurements because of structural disorder in the ligand on one-half of the molecule. [d]Calculated from the slopes of the linear portion of ln([LA]) vs time plots for the polymerization of 200 equiv *rac*-LA (0.5 M) with [cat.] = 2 mM with 1,3,5-trimethoxybenzene (0.03 M) used as an internal standard. [e]Value is for complex **4**.

the system, we attempted many routes toward the synthesis of the deuterated analogue of **1**, namely, $[(N_{Me2}N_DO)InCl]_2(\mu\text{-Cl})(\mu\text{-OEt})$. Two general strategies were used: use of $D(NN_DO)$ as the proligand and deuteration of the indium complexes. All our attempts were unsuccessful. The difficulties of this proposed synthesis originate from the facile exchange of the secondary amine proton with any protic source, as evidenced by the loss of the N*H* signal in the ^{1}H NMR spectrum of the ligand. The deuterated compounds will not be discussed further.

Polymerization Studies. Polymerization studies with complexes **2**, **6**, and **8** were carried out and compared to previously studied systems **1**,[5d] **3**,[8] **4′**,[5b] and **C**[5b] in order to determine the effects of the central amine on the reactivity of these catalysts (Table 2).

The effect of secondary vs tertiary amine donors was studied through complexes **1** and **8** vs complexes **6** and **C**, respectively. The polymerization of 200 equiv of *rac*-LA by **6** can be monitored in CD_2Cl_2 by ^{1}H NMR spectroscopy. The plot of ln([LA]) versus time shows no significant induction period, and the propagation proceeds with a k_{obs} value of 1.24×10^{-5} s^{-1} (Figure 3). The rate for **6** is 2 orders of magnitude lower than the rate for complex **1** (k_{obs} = 1.72×10^{-3} s^{-1}) under similar conditions. The ring opening polymerization of 200 equiv of *rac*-LA with **6** reaches >95% conversion in 3 days. In stark contrast, a similar reaction catalyzed by complex **1** reaches >95% conversion in 30 min.

A similar phenomenon is observed when comparing complex **8** to its methylated analogue **C**. The polymerization of 200 equiv of *rac*-LA by complex **8** proceeds to over 90% conversion in 60 min. In situ monitoring of this reaction by ^{1}H NMR spectroscopy in CD_2Cl_2 shows a short induction period, and the propagation proceeds with a k_{obs} value of 0.76×10^{-3} s^{-1} (Figure 4). This rate is 2 orders of magnitude faster than the methylated analogue **C** (k_{obs} = 1.1×10^{-5} s^{-1}) under similar conditions.[5b] This is the same trend observed with the chiral complexes **1** and **6** as discussed above.

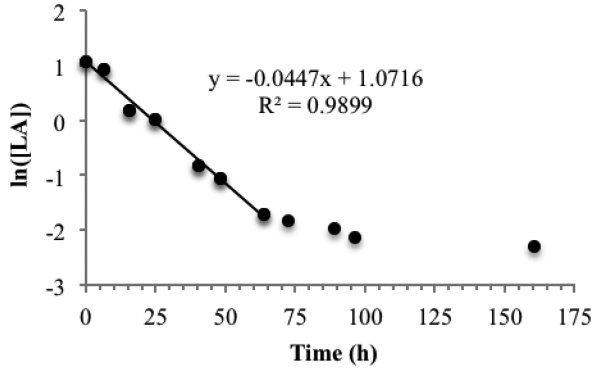

Figure 3. Plot of ln([LA]) vs time for the ROP of 200 equiv of *rac*-LA (0.47 M) with complex **6** (2.4 mM) monitored to 97% conversion by ^{1}H NMR spectroscopy (300 MHz, CD_2Cl_2, 25 °C). 1,3,5-Trimethoxybenzene was used as an internal standard.

We also compared the propagation rates of the parent chloro-substituted catalyst (**1**) to its bromo (**2**) and iodo (**3**) analogues, for which the H-bonding is weaker (Table 2). The reported rates of propagation (k_p) for **1** and an analogue of the iodo complex,

dx.doi.org/10.1021/ic501529f | Inorg. Chem. 2014, 53, 9897−9906

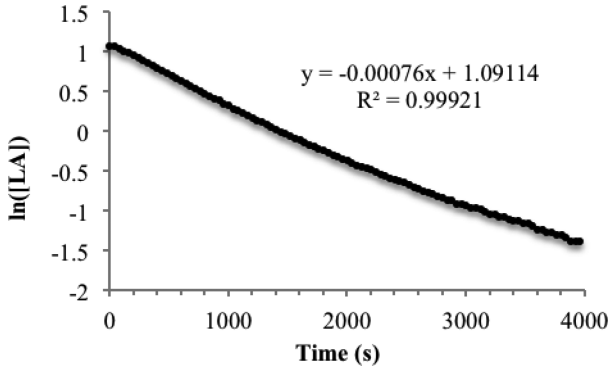

Figure 4. Plot of ln([LA]) vs time for the ROP of 200 equiv of *rac*-LA (0.50 M) with complex **8** (2.5 mM) monitored to 93% conversion by ^{1}H NMR spectroscopy (400 MHz, CD_2Cl_2, 25 °C). 1,3,5-Trimethoxybenzene was used as an internal standard.

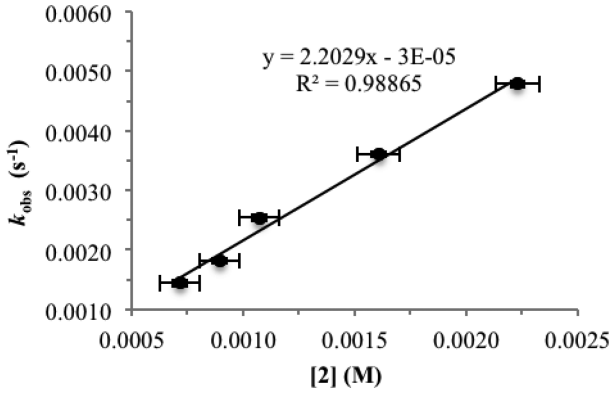

Figure 5. Plot of observed rate constants (k_{obs}) at different catalyst concentrations for the polymerization of *rac*-LA by **2**, monitored to >97% conversion by ^{1}H NMR spectroscopy (400 MHz, 25 °C, $CDCl_3$). [LA] = 0.45 M, [**2**] = 0.7, 0.9, 1.1, 1.6, and 2.2 mM with 1,3,5-trimethoxybenzene (0.033 M) used as an internal standard.

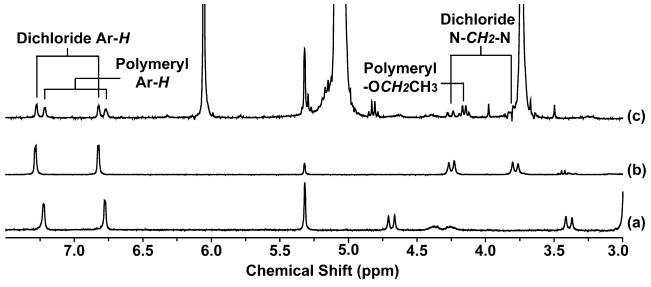

Figure 6. ^{1}H NMR spectra (300 MHz, CD_2Cl_2, 25 °C) of (a) complex **6**, (b) complex **5**, and (c) polymerization of *rac*-LA (0.47 M) with complex **6** (2.4 mM) ~10 min after preparation of the sample.

where the para-*t*Bu groups on the phenolate rings have been replaced by methyl groups, $[(N_{Me2}N_HO_{tBuMe})InI]_2(\mu\text{-}I)(\mu\text{-}OEt)$ (**3**′), are 0.57(5) and 1.50(13) M^{-1} s^{-1} respectively.[5d,8] The k_p value for the bromo complex (**2**), determined by obtaining the k_{obs} values for a range of catalyst concentrations, is 2.20(13) M^{-1} s^{-1} (Figure 5). This value is in the same range as those reported for complexes **1** and **3**′ and indicates that the much lower rates for methylated complexes **6** and **C** are true outliers in the series.

We investigated two possibilities for the significant decrease in the rate in moving from secondary to tertiary central amine donors: (1) the lack of hydrogen bonding in the system which may affect the stability of the dinuclear catalyst and lead to catalyst dissociation, and (2) the change in the electrophilicity of the metal center in moving from secondary to tertiary amines.[10a] With the complexes at hand, however, it is challenging to separate the two effects: compounds that show no hydrogen bonding are also electronically different.

In situ observation of the polymerization of *rac*-LA with complex **6** shows catalyst dissociation to the dichloride complex $(N_{Me2}N_{Me}O)InCl_2$ (**5**) and a polymeryl species immediately after preparation of the sample (Figure 6). We have previously observed a similar dissociation process with catalysts in this series that we assume have no hydrogen bonding, namely, complex **C** and the ethoxy-chloro bridged analogue of complex **4**, $[(N_{nPr2}N_HO)InCl]_2(\mu\text{-}Cl)(\mu\text{-}OEt)$ (**4**′).[5b]

In contrast, dissociation is not observed for catalyst **8**. *In situ* observation of lactide polymerization with **8** shows unreacted catalyst and a polymeryl species during the early stages of the polymerization and only the polymeryl species at the late stages of the polymerization (Figure 7). This is consistent with catalyst

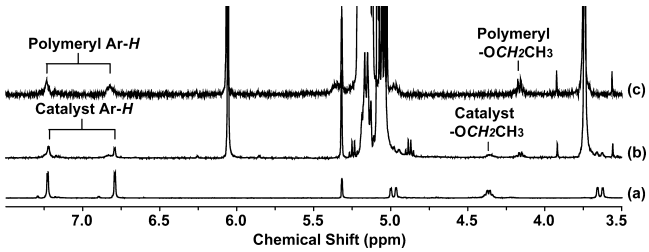

Figure 7. ^{1}H NMR spectra (400 MHz, CD_2Cl_2, 25 °C) of (a) complex **9**, (b) polymerization of *rac*-LA (0.50 M) with complex **8** (2.5 mM) ~7 min after preparation of the sample, and (c) polymerization of *rac*-LA (0.50 M) with complex **9** (2.5 mM) ~66 min after preparation of the sample.

1, where dissociation is also not observed during polymerization, and detailed mechanistic studies have revealed that a dimeric propagating species is most consistent with the observed experimental evidence.[8]

One interpretation of these results can be that a lack of H-bonding, such as in complexes **4**, **6**, and **C**, may lead to dissociation of the dimers during polymerization of lactide. However, comparison of polymerization rates suggests a more nuanced situation (Table 2). If this dissociation is responsible for the lowered activity of complexes **6** and **C**, we would expect complex **4**′ to have a similar slow rate of polymerization (if we assume the structure of complex **4**′ would be closely related to complex **4** and therefore also show a lack of H-bonding). This is not the case, however, as complex **4**′ shows a rate comparable to the parent system, with a k_{obs} value of 2.1 × 10^{-3} s^{-1}, 2 orders of magnitude higher than both complexes **6** and **C**.[5b] Also, we show that changing the halide group from chloro- to iodo-, which leads to decreased hydrogen bonding, has no major impact on the polymerization rate.

From these results, we can infer that although H-bonding may be playing a role in the stability of the dimeric structure of these types of catalysts, it is likely not a universal contributing factor in their activity toward lactide polymerization. We can then speculate that the slower rates of polymerization may be due to the difference in the electronic nature of the central metal. Complexes with tertiary amine donors, complexes **6** and **C**, show considerably slower rates compared to their secondary amine analogues, complexes **1** and **8**. To investigate the validity of this claim, we turned to DFT calculations to give us insight into the

dx.doi.org/10.1021/ic501529f | Inorg. Chem. 2014, 53, 9897−9906

Table 3. Polymerization of *rac*-LA by 2, 6, and 8

I	LA:I	T (h)	Con (%)[a]	$M_{n\ theo}$[b] (Da)	$M_{n\ GPC}$[c] (Da)	PDI	P_m[d]
2	292	24	98	41290	45700	1.05	0.59
2	395	17	98	55850	57350	1.02	
2	574	24	98	80770	82050	1.02	0.58
2	867	24	97	121690	111500	1.03	0.61
6	204	72	96	28330	23630	1.09	
6	261	144	97	36480	39500	1.02	0.44
6	620	144	71	63480	57200	1.03	
6	804	288	92	106610	85890	1.06	0.43
8	214	17	93	28710	30480	1.07	0.50
8	341	18	95	46710	49650	1.01	0.55
8	609	18	97	85170	93830	1.02	0.54
8	801	18	96	110890	114100	1.02	0.51

[a]Monomer conversion, determined by ^{1}H NMR spectroscopy. [b]Calculated from $[LA]_o/[initiator] \times$ LA conversion $\times M_{LA}$ (144.13) + M_{EtOH} (46.07). [c]Determined by GPC−LALLS (gel permeation chromatography−low angle laser light scattering) using a polystyrene standard calibration curve made via the Mark−Houwink equation in THF at 25 °C ($[\eta] = KM^a$, while $[\eta]$ = intrinsic viscosity, M = molecular weight, and K and a are the Mark−Houwink parameters, $K = 1.832 \times 10^{-4}$ dL/g, and $a = 0.69$; dn/d$c = 0.042$ mL/g). [d]Calculated from the ^{1}H{^{1}H} NMR spectra and Bernoullian statistics.

electron density at the indium center in the precatalyst and how this might be affected by the nature of the central amine donor.

DFT calculations were carried out using ORCA[15] with a B3LYP functional. The available Def2-SV(P) basis set was used for all atoms, and geometric optimizations were carried out in the gas phase. Complexes **1** and **6** were optimized in these calculations. The validity of the calculations was established by comparing the metrical parameters obtained after the optimization, with those obtained from the X-ray structures of the complexes (Table S2, Supporting Information). In order to establish whether any electronic differences can be observed at the indium centers of **1** and **6**, the partial atomic charges were determined using Mulliken population analysis and Loewden analysis. The In Mulliken charge for both **1** and **6** was 1.05, and the corresponding Loewden charges were 0.29 and 0.27. This indicates that no significant difference exists in the electronics at the indium centers in **1** and **6**.

Finally, we have analyzed the polymers generated by the various catalysts to determine whether there are differences in the systems with and without a tertiary amine donor. Bulk polymerizations of *rac*-LA with complexes **2**, **6**, and **8** with various equivalents of monomer show molecular weights (M_n) fairly consistent with theoretical values and low polydispersity (PDI) values indicative of living polymerization in all systems (Table 3). The bromo catalyst **2** shows a slight isotactic bias in selectivity with $P_m = 0.58-0.61$ and is comparable to the parent system $[(N_{Me2}N_HO)InCl]_2(\mu\text{-Cl})(\mu\text{-OEt})$ (**1**) ($P_m \approx 0.61$). In contrast, catalysts **6** ($P_m = 0.43-0.44$) and **8** ($P_m = 0.50-0.55$) show no selectivity, with P_m values consistent with the loss of isotactic bias. A similar loss in isoselectivity was observed with complex **4′**. Interestingly, these are the three compounds that definitively dissociate during polymerization, indicating that isoselectivity is imparted by the dinuclear structure.

The experimental data show that there is no real change in the catalyst performance with a change in halide, as both the activity, selectivity, and molecular weight control of the bromide catalyst $[(N_{Me2}N_HO)InBr]_2(\mu\text{-Br})(\mu\text{-OEt})$ (**2**) is comparable to the parent chloride catalyst $[(N_{Me2}N_HO)InCl]_2(\mu\text{-Cl})(\mu\text{-OEt})$ (**1**). This is similar to our previous observations with the iodo analogue $[(N_{Me2}N_HO_{tBuMe})InI]_2(\mu\text{-I})(\mu\text{-OEt})$ (**3′**), which was also shown to have a performance similar to the parent system.[8]

CONCLUSIONS

There is a profound difference in polymerization reactivity between dinuclear indium complexes supported by tridentate diaminophenolate ligands where the central amine is secondary vs tertiary. With secondary amine supports, such as in indium complexes **1**, **2**, **3**, **4′**, and **8**, the ring opening polymerization of 200 equiv of racemic lactide proceeds at room temperature in under an hour. In contrast, when the central amine is methylated, as in complexes **6** and **C**, the rate of polymerization is 2 orders of magnitude slower under the same conditions.

Our preliminary computational study of the series showed no significant change in the electronics of the indium center upon changing the central donor amine; thus we sought to gain more insight into this disparity by exploring the role of hydrogen bonding in the system. Our study shows that although there is evidence for hydrogen bonding in the chloro- and bromo substituted complexes **1** and **2**, weakening of the hydrogen bonding (larger halide **3** or bulkier analogue **4**) or removal of hydrogen bonding (methylated analogues **6** and **C**) comes with significant changes in sterics, leading to catalyst dissociation during polymerization. This dissociation does not always translate to reduced activity, with catalyst **4′** having similar reactivity to catalysts **1** and **2** and catalysts **6** and **C** being considerably slower. In systems capable of dissociation, all selectivity is lost.

Thus, it is exceedingly difficult to decouple competing electronic and steric factors in this family of catalysts and isolate hydrogen bonding as the factor impacting reactivity in the system. We can conclude that in catalysts with similar steric environments, a change of donors from tertiary to secondary amines can have a very significant impact on catalyst reactivity.

EXPERIMENTAL SECTION

General Methods. All air and/or water sensitive reactions were carried out under N_2 in an MBraun glovebox. A Bruker Avance 300 MHz or 400inv MHz spectrometer was used to record the ^{1}H NMR kinetics experiments, and a Bruker Avance 600 MHz spectrometer was used to record the ^{1}H NMR, ^{13}C{^{1}H} NMR spectra and ^{1}H{^{1}H} NMR spectra. ^{1}H NMR chemical shifts are given in ppm versus residual protons in deuterated solvents as follows: δ 5.32 for CD_2Cl_2 and 7.27 for $CDCl_3$. ^{13}C{^{1}H} NMR chemical shifts are given in ppm versus residual ^{13}C in solvents as follows: δ 54.00 for CD_2Cl_2 and 77.00 for $CDCl_3$. Diffraction measurements for X-ray crystallography were made on Bruker X8 APEX

dx.doi.org/10.1021/ic501529f | Inorg. Chem. 2014, 53, 9897−9906

II and Bruker APEX DUO diffractometers with graphite monochromated Mo Kα radiation. The structures were solved by direct methods and refined by full-matrix least-squares using the SHELXTL crystallographic software of the Bruker-AXS. Unless specified, all non-hydrogens were refined with anisotropic displacement parameters, and all hydrogen atoms were constrained to geometrically calculated positions but were not refined. EA CHN analysis was performed using Carlo Erba EA1108 elemental analyzer. The elemental composition of an unknown sample was determined by using a calibration factor. The calibration factor was determined by analyzing a suitable certified organic standard (OAS) of a known elemental composition. Molecular weights were determined by GPC-LLS using an Agilent liquid chromatograph equipped with either an Agilent 1200 series pump and autosampler, three Phenogel 5 μm Narrow Bore columns (4.6 × 300 mm with 500 Å, 10^3 Å and 10^4 Å pore size), a Wyatt Optilab differential refractometer, Wyatt tristar miniDAWN (laser light scattering detector) and a Wyatt ViscoStar viscometer or an Agilent 1200 Series pump and autosampler, Phenomenex columns (Phenogel 5 μm 10E4A LC Column 300 × 4.6 mm, 5 K − 500 K MW; Phenogel 5 μm 10E3A LC Column 300 × 4.6 mm, 1 K − 75 K MW; Phenogel 5 μm 500 ÅLC Column 300 × 4.6 mm, 1 K − 15 K MW), Wyatt Optilab rEX (refractive index detector λ = 690 nm, 40 °C), Wyatt tristar miniDAWN (laser light scattering detector operating at λ = 690 nm), and a Wyatt ViscoStar viscometer. The column temperature was set at 40 °C. A flow rate of 0.5 mL/min was used, and samples were dissolved in THF (ca. 5 mg/mL). Narrow molecular weight polystyrene standards were used for calibration purposes. An analytical balance with a maximum error value of ±0.0005 g was used for all measurements.

Toluene, diethyl ether, hexane, and tetrahydrofuran were degassed and dried using alumina columns in a solvent purification system. The THF was further dried over sodium/benzophenone and vacuum transferred to a Strauss flask where it was degassed prior to use. In addition CH_3CN and CH_2Cl_2 were dried over CaH_2 and vacuum transferred to a Strauss flask where they were degassed prior to use. Deuterated chloroform ($CDCl_3$) and dichloromethane (CD_2Cl_2) were dried over CaH_2 and vacuum transferred to a Strauss flask and then degassed through a series of freeze−pump−thaw cycles. $InCl_3$ was obtained from Strem Chemicals and $InBr_3$ was obtained from Alfa Aesar. Both were used without further purification. Benzyl potassium was synthesized using a modified literature preparation of *n*-butyl lithium, potassium *tert*-butoxide, and toluene. The ligand 2,4-di-*tert*-butyl-6-(((2-(dimethylamino)cyclohexyl)(methyl)amino)methyl)phenol **H-($N_{Me2}N_{Me}O$)**[4,11] and the bromide complex **2**[Sc] were prepared according to previously published procedures. Lactide samples were obtained from Purac Biomaterials and recrystallized several times from hot, dry toluene and dried under a vacuum prior to use.

Synthesis of Complex 5. A suspension of benzyl potassium (0.1701 g, 1.306 mmol) in toluene (10 mL) was added to a solution of **H($N_{Me2}N_{Me}O$)** (0.4906 g, 1.310 mmol) in toluene (10 mL). The reaction mixture was stirred at room temperature for 15 h, and the solvent was removed *in vacuo* to obtain **K($N_{Me2}N_{Me}O$)** as a pale yellow solid in quantitative yield. The potassium salt, **K($N_{Me2}N_{Me}O$)** (0.5801 g, 1.406 mmol) was dissolved in THF (5 mL). To this solution was added a slurry of indium trichloride (0.3103 g, 1.403 mmol) in THF (10 mL). The mixture was stirred at room temperature for 17 h and then filtered through glass fiber filter paper. The clear pale orange filtrate was concentrated *in vacuo* until a solid precipitate formed, which was then filtered *in vacuo* to obtain a pale yellow solid. The solid was recrystallized by dissolving in a minimum of THF and cooling in the freezer (−35 °C) until white crystals had formed, which were filtered *in vacuo*. The crystals were then stirred in ether for ∼30 min and filtered yielding complex **5** as a white powder, which was dried under a vacuum several hours to remove residual solvents (0.34 g, 43%). ^{1}H NMR (600 MHz, CD_2Cl_2, 25 °C): δ 7.29 (1H, d, $^4J_{HH}$ = 6 Hz, Ar*H*), 6.83 (1H, d, $^4J_{HH}$ = 6 Hz, Ar*H*), 4.25 (1H, d, $^2J_{HH}$ = 12 Hz, CH_2N), 3.78 (1H, d, $^2J_{HH}$ = 12 Hz, CH_2N), 2.80 (1H, m, C*H*N), 2.78 (3H, s, NCH_3), 2.73 (1H, m, C*H*N), 2.64 (3H, s, NCH_3), 2.20 (4H, m, DACH + NCH_3), 2.13 (1H, m, DACH), 1.92 (2H, m, DACH), 1.43 (2H, m, DACH), 1.42 (9H, s, C(CH_3)$_3$), 1.27 (9H, s, C(CH_3)$_3$), 1.24 (2H, m, DACH). ^{13}C{^{1}H} NMR (151 MHz, CD_2Cl_2, 25 °C): δ 160.73, 139.57, 139.13, 125.83, 125.26, 120.90, 63.31, 62.72, 62.42, 45.24, 39.37, 38.53, 35.50, 34.45, 31.99, 30.09, 24.84, 24.78, 23.44, 23.11. Anal. Calcd for $C_{24}H_{41}Cl_2InN_2O$: C, 51.54; H, 7.39; N, 5.01. Found: C, 51.88; H, 7.69; N, 5.00.

Synthesis of Complex 6. To a solution of complex **5** (0.2179 g, 0.3896 mmol) in THF (5 mL) was added a suspension of sodium ethoxide (0.0260 g, 0.382 mmol) in THF (5 mL). The mixture was stirred for 19 h, after which the solution had turned cloudy off-white. The solution was filtered through glass fiber filter paper, removing a significant amount of white precipitate. The clear, off-white filtrate was concentrated *in vacuo* until a white precipitate started to form (1−2 mL volume), after which ether (∼5 mL) was added. The solution was stirred for several minutes and then filtered yielding a portion of the crude product as a white powder. The precipitate from the crude reaction mixture was dissolved in DCM (∼5 mL) and filtered, and then this solution was combined with the solid obtained from THF-ether and pumped to dryness yielding a white powder. The combined solid was stirred in ether (∼5 mL) for ∼30 min, and then filtered *in vacuo* to yield the pure product as a white powder, which was dried under a vacuum for several hours to remove residual solvents (0.1531 g, 70%). Colorless needles suitable for X-ray analysis were grown from a saturated solution of the complex in acetonitrile at room temperature. ^{1}H NMR (600 MHz, $CDCl_3$, 25 °C): δ 7.24 (1H, d, Ar*H*), 6.75 (1H, d, Ar*H*), 4.75 (1H, d, $^2J_{HH}$ = 12 Hz, CH_2N), 4.41 (m, 1H, OCH_2CH$_3$), 3.38 (1H, d, $^2J_{HH}$ = 12 Hz, CH_2N), 3.03 (3H, s, NCH_3), 2.76 (1H, m, C*H*N), 2.73 (3H, s, NCH_3), 2.69 (1H, m, C*H*N), 2.24 (3H, s, NCH_3), 1.96 (2H, m, DACH), 1.79 (2H, m, DACH), 1.45 (9H, s, C(CH_3)$_3$), 1.33 (1H, m, DACH), 1.27 (9H, s, C(CH_3)$_3$), 1.25 (1.5H, m, OCH$_2$CH_3), 1.18 (2H, m, DACH), 0.96 (1H, m, DACH). ^{13}C{^{1}H} NMR (151 MHz, $CDCl_3$, 25 °C): δ 161.55, 138.42, 136.16, 125.41, 124.27, 119.03, 62.99, 62.15, 61.55, 55.88, 44.65, 42.36, 38.43, 35.18, 33.86, 31.80, 29.97, 24.48, 24.00, 22.25, 21.69, 19.78. Anal. Calcd for $C_{50}H_{87}Cl_3In_2N_4O_3$: C, 53.23; H, 7.77; N, 4.97. Found: C, 53.54; H, 7.99; N, 5.00.

Synthesis of H(L_H). The synthesis was adapted from the literature.[12] To a solution of 2,4-di-*tert*-butylsalicylaldehyde (2.135 g, 9.111 mmol) in methanol (25 mL) was added *N*,*N*-dimethylethylenediamine (0.804 g, 9.12 mmol). The solution was stirred at room temperature for 20 h, and then pumped to dryness *in vacuo* yielding the imine as a thick orange oil (2.73 g, 98%). The imine was dissolved in acetonitrile (30 mL), sodium cyanoborohydride (2.824 g, 44.94 mmol) was added, and the solution was stirred for 30 min. Acetic acid (2.5 mL, 44 mmol) was then added, and the solution was stirred at room temperature for 16 h. The mixture was diluted with 5% MeOH in DCM (50 mL) and then washed with 1 M NaOH (3 × 50 mL). The organics were dried over $MgSO_4$ and then filtered and pumped to dryness, yielding the crude product as a thick pale yellow oil (2.75 g, 100%). The oil was dissolved in hexanes, causing precipitation of a white solid. The solid was removed via filtration, and the filtrate was collected and pumped to dryness *in vacuo* yielding a purer fraction of the product as a viscous pale yellow oil. This oil was taken into the glovebox and dissolved in hexanes, and then dried over Na_2SO_4 to remove water impurities, filtered, and pumped to dryness *in vacuo* yielding a thick pale yellow oil (1.55 g, 56%). The product was used without further purification. ^{1}H NMR (600 MHz, $CDCl_3$, 25 °C): δ 7.22 (1H, d, $^4J_{HH}$ = 2 Hz, Ar*H*), 6.87 (1H, d, $^4J_{HH}$ = 2 Hz, Ar*H*), 3.97 (2H, s, ArCH_2NH), 2.74 (2H, t, $^2J_{HH}$ = 6 Hz, NHCH_2CH_2N), 2.46 (2H, t, $^2J_{HH}$ = 6 Hz, NHCH_2CH_2N), 2.24 (6H, s, N(CH_3)$_2$), 1.43 (9H, s, C(CH_3)$_3$), 1.29 (9H, s, C(CH_3)$_3$). ^{13}C{^{1}H} NMR (150 MHz, $CDCl_3$, 25 °C): δ 154.73, 140.25, 135.73, 123.09, 122.79, 122.05, 58.25, 53.39, 45.89, 45.42, 34.86, 34.11, 31.67, 29.61. Anal. Calcd for $C_{19}H_{34}N_2O$: C, 74.46; H, 11.18; N, 9.14. Found: C, 74.14; H, 11.20; N, 9.37.

Synthesis of Complex 7. To a solution of **H(L_H)** (0.5057 g, 1.650 mmol) in toluene (5 mL) was added a slurry of potassium *tert*-butoxide (0.1850 g, 1.649 mmol) in toluene (10 mL). The solution was stirred at room temperature for 22 h and then pumped to dryness *in vacuo* yielding the potassium salt as a yellow powder. This solid was stirred in hexane, filtered, and dried under a vacuum to yield the purified potassium salt as a pale off-white solid (0.4779 g). The salt (0.4779 g, 1.387 mmol) was dissolved in THF (5 mL), and a slurry of indium trichloride (0.3067 g, 1.387 mmol) in THF (10 mL) was added. The solution was stirred at

dx.doi.org/10.1021/ic501529f | *Inorg. Chem.* 2014, 53, 9897−9906

room temperature for 20 h, and then filtered through glass fiber filter paper. The crude mixture was concentrated *in vacuo* until 1−2 mL of THF remained, and then ether (5 mL) was added, causing the precipitation of a white solid. The solution was stirred for approximately 1 h, and then it was filtered on a glass frit yielding the purified product as a white solid (0.50 g, 73%). Although NMR studies did not indicate any significant impurities were present in this product, EA CHN analysis was outside the acceptable range; therefore the product was dissolved in DCM (1−2 mL) making a slightly cloudy solution. The solution was filtered through glass fiber filter paper and through Celite multiple times; however the cloudiness could not be fully removed. The solvent was removed *in vacuo* and EA CHN analysis of the resulting solid did show improved values (see below); however they were still outside the acceptable range. Because of the difficulties in removing what is assumed to be leftover NaCl byproduct from the reaction mixture, we did not seek to repeat the EA analysis and instead utilized this product without further purification. ^{1}H NMR (600 MHz, $CDCl_3$, 25 °C): δ 7.26 (1H, d, $^4J_{HH}$ = 2 Hz, Ar*H*), 6.79 (1H, d, $^4J_{HH}$ = 2 Hz, Ar*H*), 4.78 (1H, m, ArCH_2NH), 3.86 (1H, m, ArCH_2NH), 3.51 (1H, m, *NH*), 3.22 (1H, m, NHCH_2CH_2N), 3.04 (1H, m, NHCH_2CH_2N), 2.97 (1H, m, NHCH_2CH_2N), 2.69 (3H, s, N$(CH_3)_2$), 2.54 (1H, m, NHCH_2CH_2N), 2.40 (3H, s, N$(CH_3)_2$), 1.27 (9H, s, C$(CH_3)_3$), 1.46 (9H, s, C$(CH_3)_3$). ^{13}C{^{1}H} NMR (151 MHz, CD_2Cl_2, 25 °C): δ 161.65, 138.95, 137.65, 125.43, 124.61, 119.65, 57.13, 53.82, 47.68, 45.97, 41.84, 35.32, 33.95, 31.73, 30.05. Anal. Calcd for $C_{19}H_{33}Cl_2InN_2O$: C, 46.46; H, 6.77; N, 5.70. Found: C, 43.08; H, 6.21; N, 5.19.

Synthesis of Complex 8. To a solution of complex **7** (0.2052 g, 0.4178 mmol) in toluene (5 mL) was added a suspension of sodium ethoxide (0.0275 g, 0.4041 mmol) in toluene (10 mL). The solution was stirred at room temperature for 18 h, and then it was filtered through glass fiber filter paper. The crude solution was concentrated *in vacuo* until crystals of the product just began to form (1−2 mL). Hexane (∼5 mL) was added, causing the precipitation of a portion of the product as a white solid. The solution was again concentrated to 1−2 mL volume, and then more hexane (∼5 mL) was added. This process was repeated one more time, and then the whole solution was left in the freezer (−35 °C) for 30 min. The solution was filtered through a glass frit, and the purified product was collected and dried under a vacuum yielding a white solid. The solid was dissolved in ether (∼5 mL), stirred for 30 min, and then dried under a vacuum to yield the final product as a white powder (0.0555 g, 27%). Colorless crystals suitable for X-ray analysis were grown from a saturated solution of the complex in acetonitrile at room temperature. ^{1}H NMR (600 MHz, $CDCl_3$, 25 °C): δ 7.25 (1H, d, $^4J_{HH}$ = 2 Hz, Ar*H*), 6.77 (1H, d, $^4J_{HH}$ = 2 Hz, Ar*H*), 5.04 (1H, d, $^2J_{HH}$ = 12 Hz, ArCH_2NH), 4.44 (1H, m, OCH_2CH_3), 3.63 (1H, d, $^2J_{HH}$ = 12 Hz, ArCH_2NH), 3.44 (1H, m, N*H*), 3.15 (1H, m, NHCH_2CH_2N), 2.92 (2H, m, NHCH_2CH_2N), 2.61 (3H, s, N$(CH_3)_2$), 2.33 (1H, m, NHCH_2CH_2N), 2.25 (3H, s, N$(CH_3)_2$), 1.44 (9H, s, C$(CH_3)_3$), 1.31 (1.5 H, t, $^3J_{HH}$ = 9 Hz, OCH_2CH_3), 1.27 (9H, s, C$(CH_3)_3$). ^{13}C{^{1}H} NMR (151 MHz, $CDCl_3$, 25 °C): δ 162.37, 138.80, 136.70, 125.79, 124.33, 119.10, 62.81, 57.13, 54.31, 47.49, 45.95, 41.60, 35.37, 33.90, 31.78, 29.94, 19.73. Anal. Calcd for $C_{40}H_{71}Cl_3In_2N_4O_3$: C, 48.43; H, 7.21; N, 5.65. Found: C, 48.50; H, 7.11; N, 5.49.

Bulk Polymerization Procedure. To a solution of catalyst (e.g., for 200 eq. LA: 0.0046 mmol) in dichloromethane (1 mL) was added *rac*-lactide (0.133 g, 0.923 mmol) in dichloromethane (1 mL). The mixture was allowed to stir at room temperature until over 90% conversion was reached as determined by ^{1}H NMR spectroscopy. The solvent was then removed *in vacuo*, and a small portion of the crude polymer was tested for tacticity via ^{1}H{^{1}H} NMR spectroscopy (600 MHz, 25 °C, $CDCl_3$). The remaining crude polymer was redissolved in a minimum of dichloromethane (1−2 mL). Methanol (2−5 mL) was then added to this solution causing precipitation of the polymer. The solution was allowed to settle, and the supernatant solution was removed. This process was repeated 2 more times, and the resulting polymer was dried under a vacuum. The polymer was tested for the presence of remaining catalyst or monomer using ^{1}H NMR spectroscopy before being tested for molecular weight and PDI using GPC in THF.

In Situ Observations of Polymerization of *rac*-LA by 6. A stock solution of catalyst **6** (0.0110 g, 0.00975 mmol) in CD_2Cl_2 was made in a 2 mL volumetric flask, and 0.5 mL of this solution was syringed into two J-Young NMR tubes. A stock solution of *rac*-lactide (0.2732 g, 1.896 mmol) and internal standard 1,3,5-trimethoxybenzene (0.0206 g, 0.122 mmol) was made in a 2 mL volumetric flask in CD_2Cl_2, and 0.5 mL of this solution was syringed into the two J-Young tubes with the catalyst solution. The tubes were sealed and the solutions were mixed. The reactions were then followed by ^{1}H NMR spectroscopy (300 MHz, 25 °C) over the next 7 days until they reached over 97% conversion.

In Situ Observations of Polymerization of *rac*-LA by 8. A stock solution of *rac*-lactide (0.2874 g, 1.994 mmol) and internal standard 1,3,5-trimethoxybenzene (0.0195 g, 0.116 mmol) was made in a 2 mL volumetric flask using CD_2Cl_2, and 0.5 mL of this solution was syringed into two J-Young NMR tubes and frozen using a liquid N_2 cold wall. A buffer layer of CD_2Cl_2 (0.25 mL) was syringed into each tube and frozen. A stock solution of catalyst **8** (0.0099 g, 0.010 mmol) in CD_2Cl_2 was made in a 1 mL volumetric flask, and 0.25 mL of this solution was syringed into each tube and frozen. The tubes were quickly evacuated and sealed while frozen to remove N_2 gas from the headspace of the tube. The reactions were quickly warmed to room temperature before being inserted into the NMR spectrometer. The reactions were followed to over 90% conversion by ^{1}H NMR spectroscopy (400 MHz, 25 °C).

Determination of k_p Value for the Polymerization of *rac*-LA by 2. A stock solution of *rac*-lactide (0.6471 g, 4.490 mmol) and internal standard 1,3,5-trimethoxybenzene (0.0555 g, 0.330 mmol) in $CDCl_3$ was made in a 5 mL volumetric flask, and 0.5 mL of this solution was syringed into five J-Young NMR tubes (samples 1−5) and frozen with a liquid N_2 cold wall. Next a buffer layer of $CDCl_3$ was added to the tubes and frozen, with 0.25 mL, 0.18 mL, 0.12 mL, 0.10 and 0.08 mL used for samples 1−5, respectively. A stock solution of catalyst **2** (0.0220 g, 0.0178 mmol) in $CDCl_3$ was made in a 2 mL volumetric flask, and 0.25 mL, 0.32 mL, 0.38 mL, 0.40 and 0.42 mL of this solution was syringed into samples 1−5, respectively, and frozen with the liquid N_2 cold wall. The tubes were then quickly evacuated and sealed while frozen to remove N_2 from the headspace of the tube. The tubes were quickly warmed to room temperature before being inserted into the NMR spectrometer. The reactions were followed to over 97% conversion by ^{1}H NMR spectroscopy (400 MHz, 25 °C).

DFT Calculations. Density functional theory (DFT) calculations were performed using the ORCA computational software package.[15] A B3LYP functional and the available Def2-SV(P) basis set were used for all atoms and geometric optimizations were carried out in the gas-phase.[16] Initial coordinates were obtained from the X-ray structures of the compounds. Increased integration grids (GRID4), slow convergence (SlowConv), and tight SCF convergence (TightSCF) criteria were also used in the optimization. Input and output files for calculations can be obtained upon request.

■ ASSOCIATED CONTENT

Ⓢ Supporting Information

Characterization of compounds in solution (NMR spectra) and in the solid states (table of selected crystallographic parameters; molecular structure of complexes **1**, **2**, **6**, and **8**); DFT calculations; crystallographic information file. This material is available free of charge via the Internet at http://pubs.acs.org.

■ AUTHOR INFORMATION

Corresponding Author

*E-mail: mehr@chem.ubc.ca.

Notes

The authors declare no competing financial interest.

■ ACKNOWLEDGMENTS

P.M. is grateful to NSERC for funding and to Prof. Laurent Maron for preliminary DFT calculations and valuable discussion.

REFERENCES

(1) (a) Vieira, I. D.; Herres-Pawlis, S. *Eur. J. Inorg. Chem.* **2012**, *5*, 765−774. (b) Dijkstra, P. J.; Du, H. Z.; Feijen, J. *Polym. Chem.* **2011**, *2* (3), 520−527. (c) Buffet, J. C.; Okuda, J. *Polym. Chem.* **2011**, *2* (12), 2758−2763. (d) Thomas, C. M. *Chem. Soc. Rev.* **2010**, *39* (1), 165−173. (e) Sutar, A. K.; Maharana, T.; Dutta, S.; Chen, C. T.; Lin, C. C. *Chem. Soc. Rev.* **2010**, *39* (5), 1724−1746. (f) Stanford, M. J.; Dove, A. P. *Chem. Soc. Rev.* **2010**, *39* (2), 486−494. (g) Wheaton, C. A.; Hayes, P. G.; Ireland, B. J. *Dalton Trans.* **2009**, No. 25, 4832−4846. (h) Chivers, T.; Konu, J. *Comments Inorg. Chem.* **2009**, *30* (5−6), 131−176. (i) Hoogenboom, R.; Schubert, U. S. *Chem. Soc. Rev.* **2006**, *35* (7), 622−629. (j) Dechy-Cabaret, O.; Martin-Vaca, B.; Bourissou, D. *Chem. Rev.* **2004**, *104* (12), 6147−6176. (k) O'Keefe, B. J.; Hillmyer, M. A.; Tolman, W. B. *J. Chem. Soc., Dalton Trans.* **2001**, No. 15, 2215−2224. (l) Dagorne, S.; Normand, M.; Kirillov, E.; Carpentier, J. F. *Coord. Chem. Rev.* **2013**, *257* (11−12), 1869−1886.

(2) (a) Maudoux, N.; Roisnel, T.; Dorcet, V.; Carpentier, J. F.; Sarazin, Y. *Chem. Eur. J.* **2014**, *20*, 6131−6147. (b) Normand, M.; Dorcet, V.; Kirillov, E.; Carpentier, J. F. *Organometallics* **2013**, *32* (6), 1694−1709. (c) Kapelski, A.; Okuda, J. *J. Polym. Sci., Part A: Polym. Chem.* **2013**, *51* (23), 4983−4991. (d) Allan, L. E. N.; Briand, G. G.; Decken, A.; Marks, J. D.; Shaver, M. P.; Wareham, R. G. *J. Organomet. Chem.* **2013**, *736*, 55−62. (e) Normand, M.; Kirillov, E.; Roisnel, T.; Carpentier, J. F. *Organometallics* **2012**, *31* (4), 1448−1457. (f) Broderick, E. M.; Guo, N.; Vogel, C. S.; Xu, C.; Sutter, J.; Miller, J. T.; Meyer, K.; Mehrkhodavandi, P.; Diaconescu, P. L. *J. Am. Chem. Soc.* **2011**, *133* (24), 9278−9281. (g) Bompart, M.; Vergnaud, J.; Strub, H.; Carpentier, J. F. *Polym. Chem.* **2011**, *2* (8), 1638−1640. (h) Blake, M. P.; Schwarz, A. D.; Mountford, P. *Organometallics* **2011**, *30* (5), 1202−1214. (i) Pietrangelo, A.; Knight, S. C.; Gupta, A. K.; Yao, L. J.; Hillmyer, M. A.; Tolman, W. B. *J. Am. Chem. Soc.* **2010**, *132* (33), 11649−11657. (j) Hu, M. G.; Wang, M.; Zhang, P. L.; Wang, L.; Zhu, F. J.; Sun, L. C. *Inorg. Chem. Commun.* **2010**, *13* (8), 968−971. (k) Buffet, J.-C.; Okuda, J.; Arnold, P. L. *Inorg. Chem.* **2010**, *49*, 419−426. (l) Pietrangelo, A.; Hillmyer, M. A.; Tolman, W. B. *Chem. Commun.* **2009**, No. 19, 2736−2737. (m) Peckermann, I.; Kapelski, A.; Spaniol, T. P.; Okuda, J. *Inorg. Chem.* **2009**, *48* (12), 5526−5534. (n) Hsieh, I. P.; Huang, C. H.; Lee, H. M.; Kuo, P. C.; Huang, J. H.; Lee, H. I.; Cheng, J. T.; Lee, G. H. *Inorg. Chim. Acta* **2006**, *359* (2), 497−504.

(3) (a) Tschan, M. J. L.; Guo, J.; Raman, S. K.; Brule, E.; Roisnel, T.; Rager, M. N.; Legay, R.; Durieux, G.; Rigaud, B.; Thomas, C. M. *Dalton Trans.* **2014**, *43* (11), 4550−4564. (b) Scheiper, C.; Dittrich, D.; Wolper, C.; Blaser, D.; Roll, J.; Schulz, S. *Eur. J. Inorg. Chem.* **2014**, *2014* (13), 2230−2240. (c) Honrado, M.; Otero, A.; Fernandez-Baeza, J.; Sanchez-Barba, L. F.; Garces, A.; Lara-Sanchez, A.; Rodriguez, A. M. *Organometallics* **2014**, *33* (7), 1859−1866. (d) Balasanthiran, V.; Chisholm, M. H.; Choojun, K.; Durr, C. B. *Dalton Trans.* **2014**, *43* (7), 2781−2788. (e) Yu, X. F.; Zhang, C.; Wang, Z. X. *Organometallics* **2013**, *32* (11), 3262−3268. (f) Wang, H. B.; Ma, H. Y. *Chem. Commun.* **2013**, *49* (77), 8686−8688. (g) Rezayee, N. M.; Gerling, K. A.; Rheingold, A. L.; Fritsch, J. M. *Dalton Trans.* **2013**, *42* (15), 5573−5586. (h) Petrus, R.; Sobota, P. *Dalton Trans.* **2013**, *42* (38), 13838−13844. (i) Sung, C. Y.; Li, C. Y.; Su, J. K.; Chen, T. Y.; Lin, C. H.; Ko, B. T. *Dalton Trans.* **2012**, *41* (3), 953−961. (j) Sun, H. S.; Ritch, J. S.; Hayes, P. G. *Dalton Trans.* **2012**, *41* (13), 3701−3713. (k) Song, S. D.; Zhang, X. Y.; Ma, H. Y.; Yang, Y. *Dalton Trans.* **2012**, *41* (11), 3266−3277. (l) Song, S. D.; Zhang, X. Y.; Ma, H. Y.; Yang, Y. *Dalton Trans.* **2012**, *41* (48), 14712−14712. (m) Roberts, C. C.; Barnett, B. R.; Green, D. B.; Fritsch, J. M. *Organometallics* **2012**, *31* (11), 4133−4141. (n) Darensbourg, D. J.; Karroonnirun, O.; Wilson, S. J. *Inorg. Chem.* **2011**, *50* (14), 6775−6787. (o) Darensbourg, D. J.; Karroonnirun, O. *Macromolecules* **2010**, *43* (21), 8880−8886. (p) Darensbourg, D. J.; Karroonnirun, O. *Inorg. Chem.* **2010**, *49* (5), 2360−2371. (q) Yu, X. F.; Wang, Z. X. *Dalton Trans.* **2013**, *42* (11), 3860−3868. (r) Sumrit, P.; Hormnirun, P. *Macromol. Chem. Phys.* **2013**, *214* (16), 1845−1851. (s) Miranda, M. O.; DePorre, Y.; Vazquez-Lima, H.; Johnson, M. A.; Marell, D. J.; Cramer, C. J.; Tolman, W. B. *Inorg. Chem.* **2013**, *52* (23), 13692−13701. (t) Hancock, S. L.; Mahon, M. F.; Jones, M. D. *Dalton Trans.* **2013**, *42* (25), 9279−9285. (u) Han, H. L.; Liu, Y.; Liu, J. Y.; Nomura, K.; Lia, Y. S. *Dalton Trans.* **2013**, *42* (34), 12346−12353. (v) Gao, B.; Duan, R. L.; Pang, X.; Li, X.; Qu, Z.; Tang, Z. H.; Zhuang, X. L.; Chen, X. S. *Organometallics* **2013**, *32* (19), 5435−5444. (w) Cross, E. D.; Allan, L. E. N.; Decken, A.; Shaver, M. P. *J. Polym. Sci., Part A: Polym. Chem.* **2013**, *51* (5), 1137−1146. (x) Bakewell, C.; White, A. J. P.; Long, N. J.; Williams, C. K. *Inorg. Chem.* **2013**, *52* (21), 12561−12567. (y) Matsubara, K.; Terata, C.; Sekine, H.; Yamatani, K.; Harada, T.; Eda, K.; Dan, M.; Koga, Y.; Yasuniwa, M. *J. Polym. Sci., Part A: Polym. Chem.* **2012**, *50* (5), 957−966. (z) Chen, H. L.; Dutta, S.; Huang, P. Y.; Lin, C. C. *Organometallics* **2012**, *31* (5), 2016−2025. (aa) Whitelaw, E. L.; Loraine, G.; Mahon, M. F.; Jones, M. D. *Dalton Trans.* **2011**, *40* (43), 11469−11473. (ab) Otero, A.; Lara-Sanchez, A.; Fernandez-Baeza, J.; Alonso-Moreno, C.; Castro-Osma, J. A.; Marquez-Segovia, I.; Sanchez-Barba, L. F.; Rodriguez, A. M.; Garcia-Martinez, J. C. *Organometallics* **2011**, *30* (6), 1507−1522. (ac) Ma, W. A.; Wang, Z. X. *Organometallics* **2011**, *30* (16), 4364−4373. (ad) Li, C. Y.; Tsai, C. Y.; Lin, C. H.; Ko, B. T. *Dalton Trans.* **2011**, *40* (9), 1880−1887. (ae) Thibault, M. H.; Fontaine, F. G. *Dalton Trans.* **2010**, *39* (24), 5688−5697. (af) Schwarz, A. D.; Chu, Z. Y.; Mountford, P. *Organometallics* **2010**, *29* (5), 1246−1260. (ag) Qian, F.; Liu, K. Y.; Ma, H. Y. *Dalton Trans.* **2010**, *39* (34), 8071−8083. (ah) Phomphrai, K.; Chumsaeng, P.; Sangtrirutnugul, P.; Kongsaeree, P.; Pohmakotr, M. *Dalton Trans.* **2010**, *39* (7), 1865−1871. (ai) Liu, Z. Z.; Gao, W.; Zhang, J. S.; Cui, D. M.; Wu, Q. L.; Mu, Y. *Organometallics* **2010**, *29* (22), 5783−5790. (aj) Liu, Z.; Gao, W.; Zhang, J.; Cui, D.; Wu, Q.; Mu, Y. *Organometallics* **2010**, *29* (22), 5783−5790. (ak) Bouyahyi, M.; Roisnel, T.; Carpentier, J. F. *Organometallics* **2010**, *29* (2), 491−500. (al) Alaaeddine, A.; Thomas, C. M.; Roisnel, T.; Carpentier, J. F. *Organometallics* **2009**, *28* (5), 1469−1475. (am) Zhang, C.; Wang, Z. X. *J. Organomet. Chem.* **2008**, *693* (19), 3151−3158. (an) Drouin, F.; Oguadinma, P. O.; Whitehorne, T. J. J.; Prud'homme, R. E.; Schaper, F. *Organometallics* **2010**, *29* (9), 2139−2147.

(4) Labourdette, G.; Lee, D. J.; Patrick, B. O.; Ezhova, M. B.; Mehrkhodavandi, P. *Organometallics* **2009**, *28* (5), 1309−1319.

(5) (a) Xu, C.; Yu, I.; Mehrkhodavandi, P. *Chem. Commun.* **2012**, *48* (54), 6806−6808. (b) Osten, K. M.; Yu, I.; Duffy, I. R.; Lagaditis, P. O.; Yu, J. C. C.; Wallis, C. J.; Mehrkhodavandi, P. *Dalton Trans.* **2012**, *41* (26), 8123−8134. (c) Acosta-Ramirez, A.; Douglas, A. F.; Yu, I.; Patrick, B. O.; Diaconescu, P. L.; Mehrkhodavandi, P. *Inorg. Chem.* **2010**, *49* (12), 5444−5452. (d) Douglas, A. F.; Patrick, B. O.; Mehrkhodavandi, P. *Angew. Chem., Int. Ed.* **2008**, *47* (12), 2290−2293.

(6) Williams, C. K.; Breyfogle, L. E.; Choi, S. K.; Nam, W.; Young, V. G.; Hillmyer, M. A.; Tolman, W. B. *J. Am. Chem. Soc.* **2003**, *125* (37), 11350−11359.

(7) (a) Aluthge, D. C.; Yan, E. X.; Ahn, J.-M.; Mehrkhodavandi, P. *Inorg. Chem.* **2014**, *53* (13), 6828−6836. (b) Aluthge, D. C.; Xu, C. L.; Othman, N.; Noroozi, N.; Hatzikiriakos, S. G.; Mehrkhodavandi, P. *Macromolecules* **2013**, *46* (10), 3965−3974. (c) Aluthge, D. C.; Patrick, B. O.; Mehrkhodavandi, P. *Chem. Commun.* **2013**, *49* (39), 4295−4297.

(8) Yu, I.; Acosta-Ramirez, A.; Mehrkhodavandi, P. *J. Am. Chem. Soc.* **2012**, *134* (30), 12758−12773.

(9) Fang, J.; Yu, I.; Mehrkhodavandi, P.; Maron, L. *Organometallics* **2013**, *32*, 6950−6956.

(10) (a) Meyerstein, D. *Coord. Chem. Rev.* **1999**, *185*−*6*, 141−147. (b) Namuswe, F.; Hayashi, T.; Jiang, Y. B.; Kasper, G. D.; Sarjeant, A. A. N.; Moenne-Loccoz, P.; Goldberg, D. P. *J. Am. Chem. Soc.* **2010**, *132* (1), 157−167. (c) Baratta, W.; Ballico, M.; Del Zotto, A.; Herdtweck, E.; Magnolia, S.; Peloso, R.; Siega, K.; Toniutti, M.; Zangrando, E.; Rigo, P. *Organometallics* **2009**, *28* (15), 4421−4430. (d) Strautmann, J. B. H.; George, S. D.; Bothe, E.; Bill, E.; Weyhermuller, T.; Stammler, A.; Bogge, H.; Glaser, T. *Inorg. Chem.* **2008**, *47* (15), 6804−6824. (e) Sreedaran, S.; Bharathi, K. S.; Rahiman, A. K.; Rajesh, K.; Nirmala, G.; Narayanan, V. *J. Coord. Chem.* **2008**, *61* (22), 3594−3609. (f) Di Bernardo, P.; Melchior, A.; Portanova, R.; Tolazzi, M.; Zanonato, P. L. *Coord. Chem. Rev.* **2008**, *252* (10−11), 1270−1285. (g) Derossi, S.; Farrell, D. T.; Harding, C. J.; McKee, V.; Nelson, J. *Dalton Trans.* **2007**, *18*, 1762−1772. (h) Del Piero, S.; Melchior, A.; Polese, P.; Portanova, R.; Tolazzi, M. *Eur. J. Inorg. Chem.* **2006**, *2*, 304−313. (i) Berry, J. F.; Bill, E.; Garcia-Serres, R.; Neese, F.; Weyhermuller, T.; Wieghardt, K. *Inorg. Chem.* **2006**, *45* (5), 2027−2037. (j) Cole, A. P.; Mahadevan, V.; Mirica,

L. M.; Ottenwaelder, X.; Stack, T. D. P. *Inorg. Chem.* **2005**, *44* (21), 7345−7364. (k) Mirica, L. M.; Vance, M.; Rudd, D. J.; Hedman, B.; Hodgson, K. O.; Solomon, E. I.; Stack, T. D. P. *J. Am. Chem. Soc.* **2002**, *124* (32), 9332−9333.
(11) Mitchell, J. M.; Finney, N. S. *Tetrahedron Lett.* **2000**, *41* (44), 8431−8434.
(12) Judmaier, M. E.; Sala, C. H.; Belaj, F.; Volpe, M.; Mosch-Zanetti, N. C. *New J. Chem.* **2013**, *37* (7), 2139−2149.
(13) Brammer, L.; Bruton, E. A.; Sherwood, P. *Cryst. Growth Des.* **2001**, *1* (4), 277−290.
(14) (a) Steiner, T. *Acta Crystallogr., Sect. B: Struct. Sci.* **1998**, *54*, 456−463. (b) Sony, S. M. M.; Ponnuswamy, M. N. *Bull. Chem. Soc. Jpn.* **2006**, *79* (11), 1766−1772.
(15) Neese, F. *ORCA—An Ab Initio, Density Functional and Semiempirical Program Package (v. 2.6−35)*; Universitat Bonn: Bonn, Germany, 2007.
(16) (a) Becke, A. D. *J. Chem. Phys.* **1993**, *98* (7), 5648−5652. (b) Stephens, P. J.; Devlin, F. J.; Chabalowski, C. F.; Frisch, M. J. *J. Phys. Chem.* **1994**, *98* (45), 11623−11627. (c) Lee, C. T.; Yang, W. T.; Parr, R. G. *Phys. Rev. B* **1988**, *37* (2), 785−789.